

## Article

# Effect of Stress on Variations in the Magnetic Field of Ferromagnetic Steel under a Constant DC Magnetic Field

Bin Yang<sup>1,2</sup>, Yang Gao<sup>2,\*</sup>, Lin Liu<sup>3</sup> , Zhifeng Liu<sup>1,\*</sup>, Yue Yu<sup>4</sup> and Ruimin Wang<sup>3</sup><sup>1</sup> School of Mechanical Engineering, Hefei University of Technology, Hefei 230002, China<sup>2</sup> School of Mechanical Engineering, North Minzu University, Yinchuan 750021, China<sup>3</sup> Mechanical Engineering Department, University of Kansas, Lawrence, KS 66045, USA<sup>4</sup> School of Electrical and Information Engineering, North Minzu University, Yinchuan 750021, China

\* Correspondence: 2008034@nmu.edu.cn (Y.G.); zhfliuhfut@126.com (Z.L.)

**Abstract:** In this paper, variations in the normal component of the magnetic field  $B_z$  on the surface of Q195 steel specimens produced by simultaneous application of noncoaxial DC magnetic field and stress were studied by tensile tests. It was found that there was no shift in the direction of  $B_z$  variations when the specimens were magnetized parallel to stress, whereas the direction of  $B_z$  variations shifted a slight angle relative to the DC magnetic field when the specimens were magnetized perpendicular to stress. The amplitude of  $B_z$  increased with stress from 0 MPa to 120 MPa when the stress was parallel to the DC magnetic field. On the contrary, the amplitude of  $B_z$  decreased with stress from 0 MPa to 120 MPa when the stress was perpendicular to the DC magnetic field. The mechanisms underlying the experimental characteristics are also discussed. This research provides the possibility for quantitative inspection of the stress in ferromagnetic steels using surface magnetic field measurements.

**Keywords:** stress; normal component of surface magnetic field; magnetization; magneto-mechanical effect



**Citation:** Yang, B.; Gao, Y.; Liu, L.; Liu, Z.; Yu, Y.; Wang, R. Effect of Stress on Variations in the Magnetic Field of Ferromagnetic Steel under a Constant DC Magnetic Field. *Energies* **2022**, *15*, 9363. <https://doi.org/10.3390/en15249363>

Academic Editors: Anna Richelli and Andrea Mariscotti

Received: 7 November 2022

Accepted: 8 December 2022

Published: 10 December 2022

**Publisher's Note:** MDPI stays neutral with regard to jurisdictional claims in published maps and institutional affiliations.



**Copyright:** © 2022 by the authors. Licensee MDPI, Basel, Switzerland. This article is an open access article distributed under the terms and conditions of the Creative Commons Attribution (CC BY) license (<https://creativecommons.org/licenses/by/4.0/>).

## 1. Introduction

It is well known that the magnetic properties of a ferromagnetic material will be altered resulting from the application of stress, which produces the so-called magneto-mechanical effect. The magneto-mechanical effect is gaining increased attention due to its potential in stress evaluation of ferromagnetic materials. Many theories [1–3] and mathematical models [4–8] have been developed to describe the magneto-mechanical effect. However, there is still a lack of systematic experimental data to study the coupling relationship between the surface magnetic field and stress of ferromagnetic materials, especially when stress and the external magnetic field are noncoaxial. It is possible to evaluate the stress inside a ferromagnetic material if the relationship can be clarified.

There have been widespread efforts to study the influences of stress on magnetic properties under the co-applied magnetic field. Craik and Wood [9] researched the magnetization changes induced by stress coaxial with a constantly applied field of various magnetic materials and obtained the magnetization-stress curve, then, a possible explanation of the curve behavior was put forward based on discontinuous changes in domain structure. S Bao [10] studied variations in the residual magnetic field on the surface of a low-carbon steel under tensile stress and geomagnetic field, and the author observed that the stress-induced magnetic fields demonstrated different characteristics in different loading stages. Previous research [11,12] has mainly focused on the special case where a magnetic field was coaxial with stress, but the field and stress axes are noncoaxial in general cases. In addition the researchers have always analyzed the magneto-mechanical effect by measuring the residual magnetic field of the stray field after stress unloading or experiments have been performed by measuring the surface magnetic field under a geomagnetic field [13–15]. In fact, it is better to measure the stray field during the tensile process because the stray field of ferromagnetic materials changes all the time during the tensile process, and these

variations can provide a better reflection of the magneto-mechanical effect. In addition, the stray field signal is easily affected by the experimental environment without an external magnetic field, resulting in inaccurate measurement results.

In this research, tensile tests of Q195 low-carbon steel specimens are performed. The normal components of magnetic field  $B_z$  on the surface of specimens are measured under a constant DC magnetic field throughout the tensile process. The DC magnetic field is provided by using a U-shaped electromagnet. The direction of the applied DC magnetic field can be changed by rotating the poles of the electromagnet, in turn, in different directions to provide noncoaxial magnetic fields. Distribution of  $B_z$  variations and the relationship between applied stress and  $B_z$  at different angles between the DC magnetic field and stress are discussed.

## 2. Materials and Methods

The tested material is Q195 low-carbon steel, which is a typical ferromagnetic material widely used in railroad tracks, nuclear power, boiler, and pipes. The chemical composition and mechanical properties of the steel are given in Table 1.

**Table 1.** Chemical composition (wt.%) and mechanical properties of Q195 steel.

Material	C	Mn	Si	S	P	Yield Strength, $\sigma_s$ (MPa)	Ultimate Tensile Strength, $\sigma_b$ (MPa)
Q195	0.06–0.12	0.25–0.50	$\leq 0.30$	$\leq 0.05$	$\leq 0.045$	195	315–430

The research steel specimens, with a thickness of 3 mm, were machined into standard sheets, as shown in Figure 1. In order to reduce the effects of the shape boundary of specimens and the poles of the electromagnet on the measurement results, the measurement area was selected in the middle area of the specimen, and occupied an area of 20 mm  $\times$  20 mm. The X and Y axis of the coordinate system are along the width direction and the length direction of the specimen, respectively. The specimens were annealed to reduce residual stress by heating them at 650 °C for two hours, and then they were allowed to cool naturally in the furnace. All the specimens were demagnetized using a demagnetizer before the magnetization tests and the tensile tests were carried out to ensure the same initial conditions.

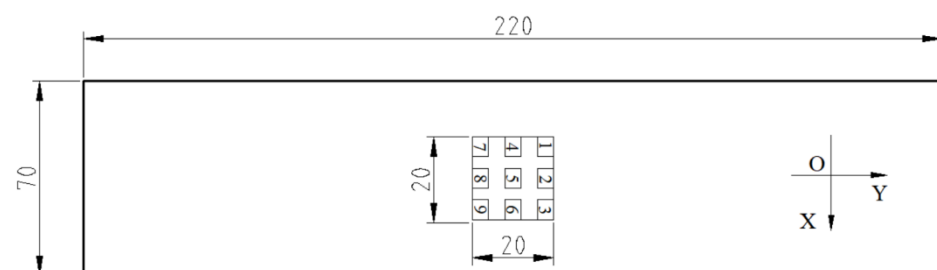


**Figure 1.** Dimensions of a specimen (in mm) and measuring area.

The detailed process of the experiment is presented as follows:

Firstly, four identical specimens were magnetized by using a U-shaped electromagnet without loading to analyze the distribution of the surface magnetic field under the DC magnetic field applied at angles of 0°, 90°, 180°, and 270°, sequentially, before the tensile tests.

Secondly, another four identical specimens were prepared for tensile tests. A continuous stress in a range from 0 MPa to 120 MPa was applied to the longitudinal axis of the specimens at a strain rate of 0.5 mm/min using an MTS testing machine with a peak capacity of 100 kN. During the tensile testing, the specimens were magnetized with a constant DC magnetic field produced using a U-shaped electromagnet about 3200 A/m at

angles of  $0^\circ$ ,  $90^\circ$ ,  $180^\circ$ , and  $270^\circ$ . The direction of the applied DC magnetic field could be changed by rotating the poles of the electromagnet, as shown in Figure 2.

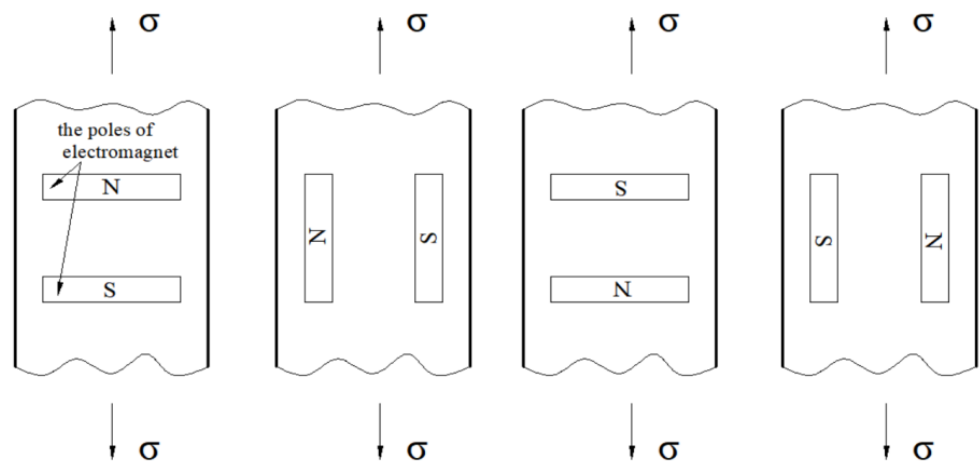


**Figure 2.** Position of the U-shaped electromagnet on a test specimen, at  $\theta = 0^\circ$ ,  $90^\circ$ ,  $180^\circ$ , and  $270^\circ$ .

During the tensile testing, the normal components of the magnetic field  $B_z$  on the surface of specimens were measured on-line using a sensor plate arranged on the other side of the specimens, the key parts of the plate are 9 magnetic probes based on TMR sensors, as shown in Figure 3. Please note that the probe output is negative for the N pole and positive for the S pole. The sensitivity of the magnetic probe was  $2.2 \text{ mV/V/Gs}$ .

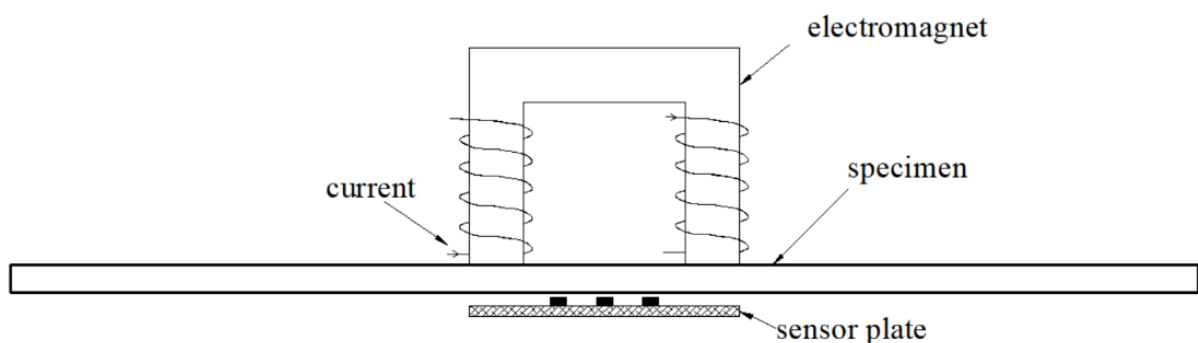


**Figure 3.** Sketch of the measurement.

Finally, the variations of  $B_z$  magnetic signals under the DC magnetic field and stress axes are noncoaxial in general cases at angles of  $22.5^\circ$ ,  $45^\circ$ , and  $67.5^\circ$  were also discussed. The test system is shown in Figure 4.

Figure 5 presents the  $B_z$  distribution on the surface of the unloaded specimens under the DC magnetic field applied at angles of  $0^\circ$ ,  $90^\circ$ ,  $180^\circ$ , and  $270^\circ$  to the stress axis. One can observe that  $B_z$  of the specimens is in the opposite direction, and the amplitude is about 1 mT when the DC magnetic field is applied at  $0^\circ$  and  $180^\circ$ . Similarly, the direction of  $B_z$  of the specimen is the opposite when the DC magnetic field is applied at  $90^\circ$  and  $270^\circ$ . Still, the amplitude is about 0.6 mT, which is less than that in  $0^\circ$  and  $180^\circ$ . In addition, the magnetic pole position of the magnetic field on the surface of the measured area is the same as that of the electromagnet when the DC magnetic field is applied at  $0^\circ$  and  $180^\circ$ , but it is reversed at  $90^\circ$  and  $270^\circ$ , namely, the probe output is positive in the measured region near the N-pole of the electromagnet.

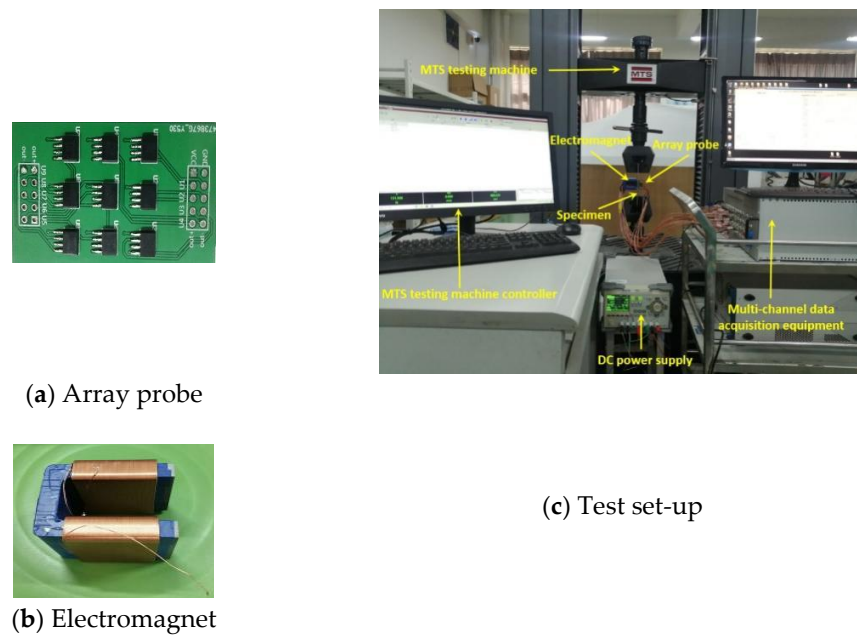
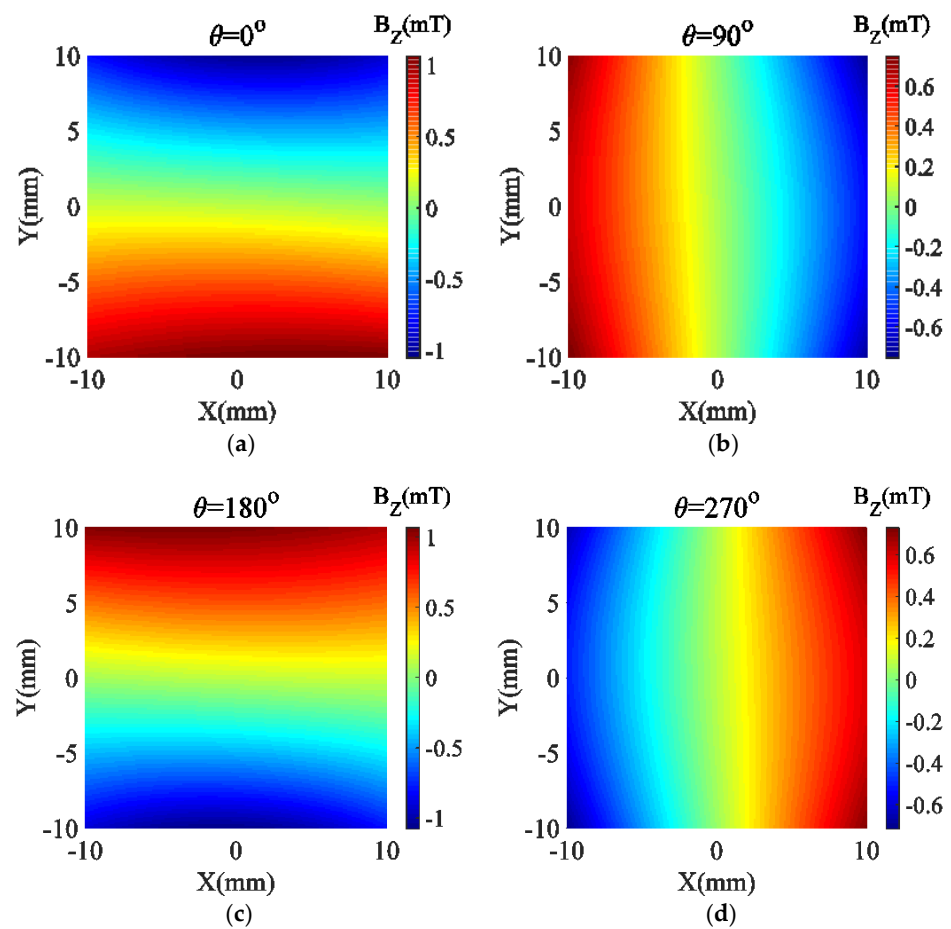


Figure 4. Test system.

Figure 5.  $B_z$  distribution of the unloaded specimens under the DC magnetic field was applied at angles of (a)  $0^\circ$ ; (b)  $90^\circ$ ; (c)  $180^\circ$ ; (d)  $270^\circ$ .

The possible reason for such a phenomenon is attributed to the shape and dimensions of the specimen. It is well known that a demagnetization field will be generated when the specimen is magnetized, and this can be described by:

$$H_d = -NM, \quad (1)$$

where  $N$  is the demagnetization factor related to the geometric shape and size of the specimen [16].

For a strip specimen, the demagnetization factor along the length direction is small [17], therefore, the demagnetization field is small when the DC magnetic field is applied at  $0^\circ$  and  $180^\circ$ . On the contrary, the demagnetization factor is larger along the width direction, and therefore, the demagnetization field is larger when the DC magnetic field is applied at  $90^\circ$  and  $270^\circ$ . In addition, the magnetization is related to the thickness of the specimen; the farther away from the magnetized surface and the poles of the electromagnet, the lower the magnetic flux density will be, as shown in Figure 6. The magnetization of the measured area is greater than the demagnetization field when the DC magnetic field is applied at  $0^\circ$  and  $180^\circ$ , therefore, the magnetic pole is the same as that of the electromagnet. On the contrary, the magnetization of the measured area is less than the demagnetization field when the DC magnetic field is  $90$  and  $270$  degrees, and therefore, the magnetic pole is opposite to the electromagnet. The amplitude of surface magnetic field intensity at  $0^\circ$  and  $180^\circ$  is greater than that at  $90^\circ$  and  $270^\circ$  because of the demagnetization field.

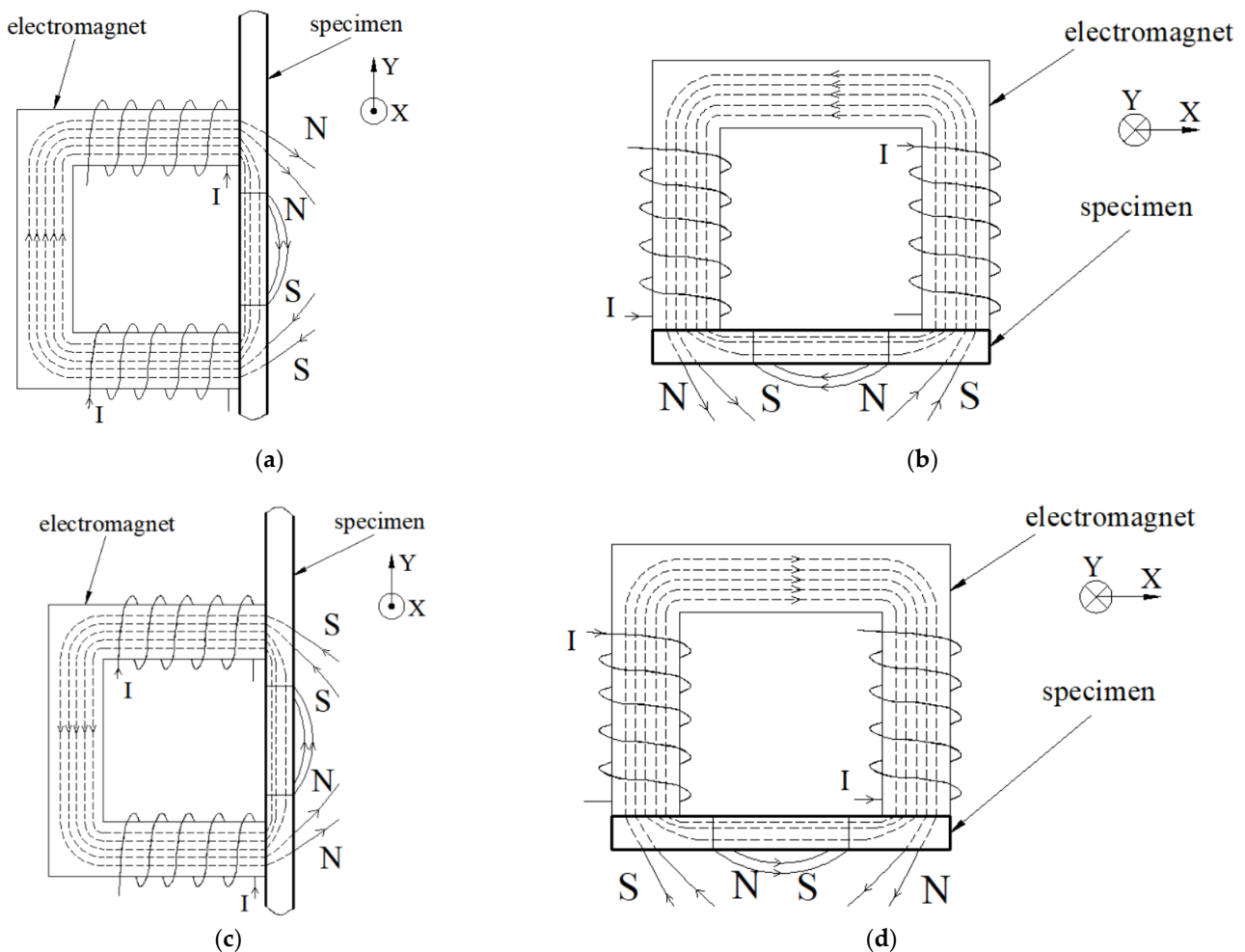


**Figure 6.** Distribution of the magnetic flux and magnetic pole of the measured area when the angle between the DC magnetic field and stress is: (a)  $0^\circ$ ; (b)  $90^\circ$ ; (c)  $180^\circ$ ; (d)  $270^\circ$ .

Figure 7 shows the change in magnetic signals of  $B_Z$  relative to stress  $\sigma$  under the DC magnetic field when applied at angles of  $0^\circ$ ,  $90^\circ$ ,  $180^\circ$  and  $270^\circ$  to the stress axis. Only the results of Probe 8 (numbered in Figure 2) are discussed. One can observe that the  $B_Z$  magnetic signal increases slightly with an increase in stress from 0 MPa to 120 MPa when the angle between the DC magnetic field and stress is  $0^\circ$  and  $180^\circ$ , and decreases with an increase in stress when the angle between the DC magnetic field and stress is  $90^\circ$  and  $270^\circ$ . Interestingly, the  $B_Z$  magnetic signal reverses to the initial signal value when the angle between the DC magnetic field and the stress is  $90^\circ$  and  $270^\circ$  under stress exceeding 100 MPa. It is known that the magnetic properties of a ferromagnetic material will be changed resulting from the internal magnetic domain structure reorganization by the wall's movement and the magnetic moment rotation under the application of mechanical stress, and bulk magnetization can become easier along the direction of tensile stress [18]. When stress is applied coaxially with the DC magnetic field (the field is applied at  $0^\circ$  and  $180^\circ$  to the stress axis), magnetization is increased because the two factors have the same effect. When stress is applied noncoaxially with the DC magnetic field (the field is applied at  $90^\circ$  and  $270^\circ$  to the stress axis), the magnetic domain walls move first, and then the magnetic moments start to rotate their orientation toward the easy magnetization direction, the magnetization is decreasing as the tensile stress is increasing.

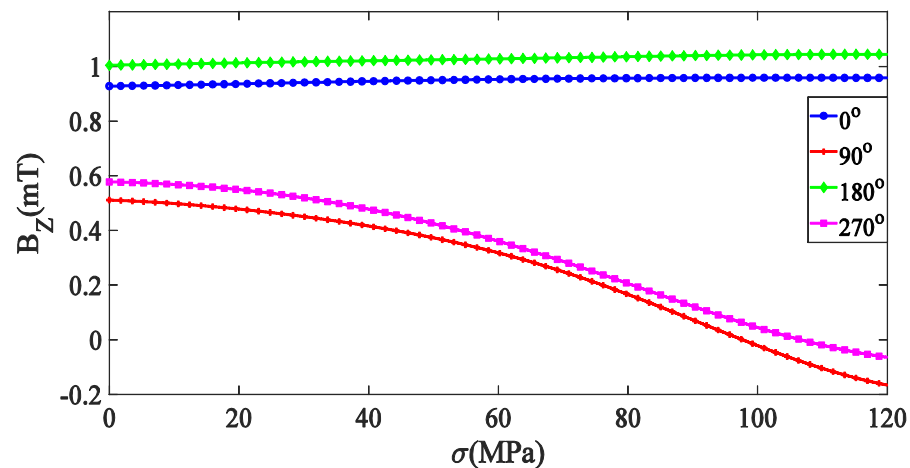
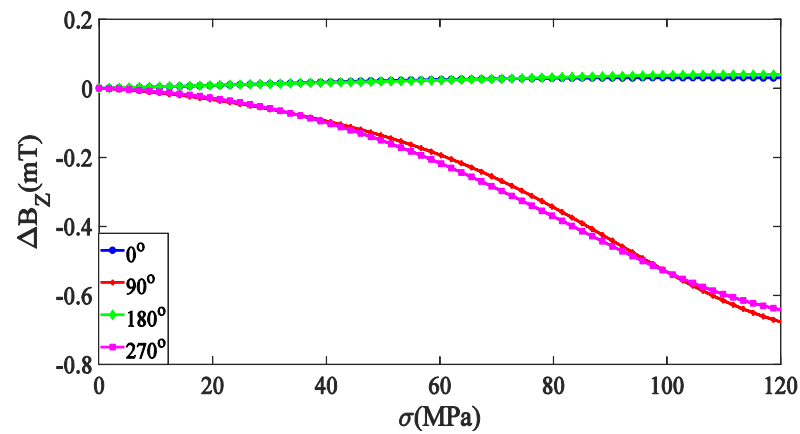


Figure 7. Changes in magnetic signals of  $B_Z$  relative to stress  $\sigma$  at angles of  $0^\circ$ ,  $90^\circ$ ,  $180^\circ$ , and  $270^\circ$ .

As can be seen in Figure 7, the initial values of  $B_Z$  magnetic signals at  $0^\circ$  and  $180^\circ$  are not equal because of the influence of the initial field such as the earth's field, nor are they equal at  $90^\circ$  and  $270^\circ$ . To eliminate its influence, we considered the initial values  $B_{Z0}$  and those after loading  $B_Z$ , i.e.,  $\Delta B_Z = B_Z - B_{Z0}$ . The results after data processing are shown in Figure 8. One may observe that variations of  $B_Z$  increase by 0.03 mT with increases in stress from 0 MPa to 120 MPa when the DC magnetic field is applied at  $0^\circ$  and  $180^\circ$  to the stress axis, and are reduced by 0.68 mT with increases in stress from 0 MPa to 120 MPa when the DC magnetic field is applied at  $90^\circ$  and  $270^\circ$  to the stress axis. The variations in  $B_Z$  are basically the same when the angle between the DC magnetic field and stress is  $0^\circ$  and  $180^\circ$ , where the DC magnetic field and stress are coaxial. Similarly, the variations in  $B_Z$  are basically the same when the angles between the DC magnetic field and stress are  $90^\circ$  and  $270^\circ$ , where the DC magnetic field and stress are noncoaxial. The reason for this phenomenon is that the specimen is subjected to a pair of uniaxial stresses of equal size and opposite direction, and therefore, the effect is the same as under the DC magnetic field applied at  $0^\circ$  and  $180^\circ$ , and the same as  $90^\circ$  and  $270^\circ$ . Stress parallel to the DC magnetic field has relatively little effect on the  $B_Z$  magnetic signals, but stress perpendicular to the DC magnetic field reduces the  $B_Z$  magnetic signals considerably.



**Figure 8.** Variations of  $B_z$  relative to stress  $\sigma$  at angles of  $0^\circ$ ,  $90^\circ$ ,  $180^\circ$ , and  $270^\circ$ , after eliminating the influence of the initial field.

Figure 9 demonstrates the distribution of the surface magnetic field variations when the DC magnetic field was applied at  $0^\circ$ ,  $90^\circ$ ,  $180^\circ$ , and  $270^\circ$  to the stress axis, under stress of 60 MPa. One can observe that there was no shift in the direction of the surface magnetic field variations when the specimen was magnetized parallel to the direction of the stress ( $0^\circ$  and  $180^\circ$ ), whereas the direction of the surface magnetic field variations shifted a slight angle relative to the DC magnetic field when the specimen was magnetized perpendicular to the direction of the stress ( $90^\circ$  and  $270^\circ$ ).

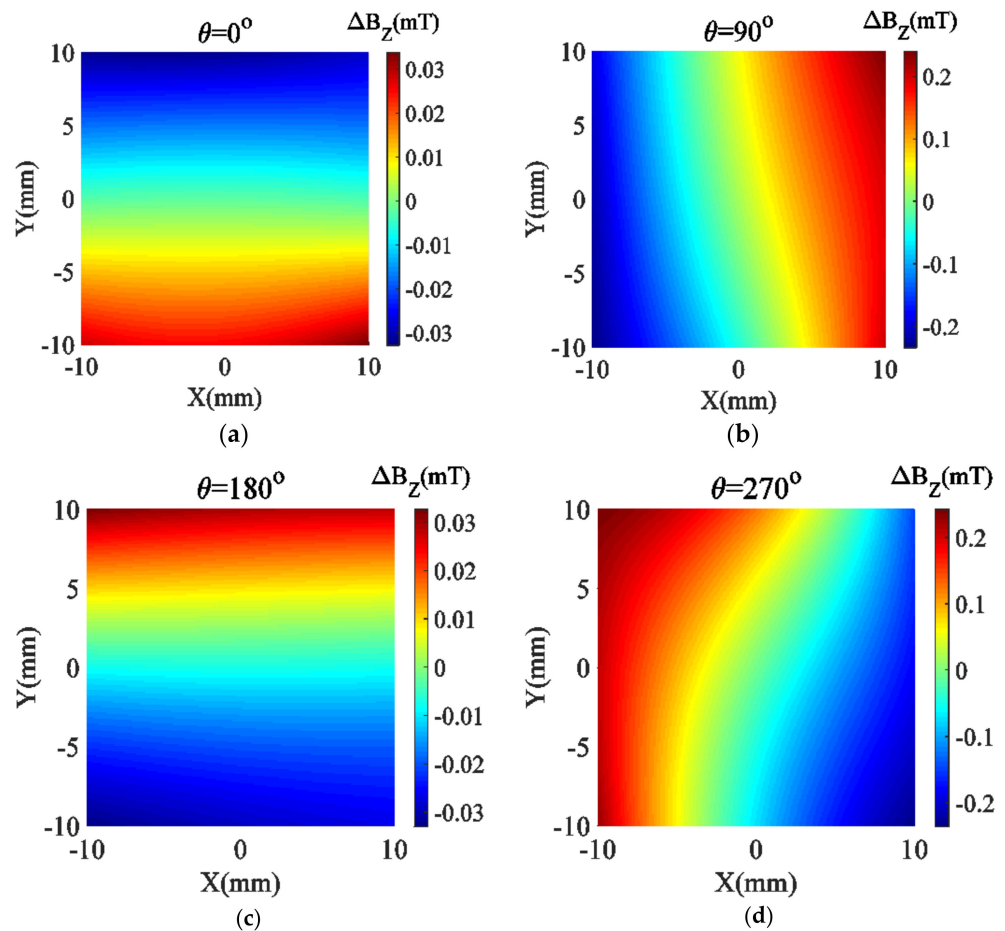


**Figure 9.** Distribution of  $\Delta B_z$  when the angle between the DC magnetic field and stress is: (a)  $0^\circ$ ; (b)  $90^\circ$ ; (c)  $180^\circ$ ; (d)  $270^\circ$  under stress of 60 MPa.

In order to study the DC magnetic field and stress axes are noncoaxial in general cases, the variations in  $B_Z$  relative to stress under the DC magnetic field applied at angles of  $0^\circ$ ,  $22.5^\circ$ ,  $45^\circ$ ,  $67.5^\circ$ , and  $90^\circ$  to the stress axis were also studied; the results are shown in Figure 10. It indicates that the variations in  $B_Z$  increase with the stress load from 0 MPa to 120 MPa at angles of  $0^\circ$ ,  $22.5^\circ$ ,  $45^\circ$ , and  $67.5^\circ$ , and reach a maximum value at  $45^\circ$ . By contrast, the variations in  $B_Z$  decrease at an angle of  $90^\circ$ . This behavior could be attributed to the easy magnetization axis of the specimen in the direction of  $45^\circ$ .

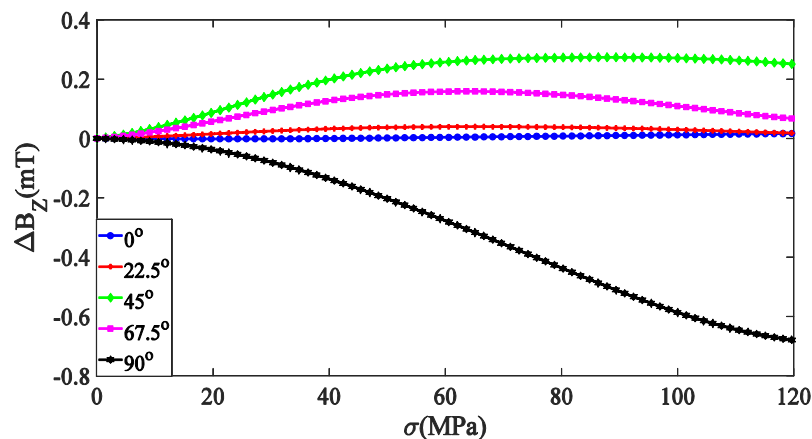


Figure 10. Variations in  $B_Z$  relative to stress  $\sigma$  at angles of  $0^\circ$ ,  $22.5^\circ$ ,  $45^\circ$ ,  $67.5^\circ$ , and  $90^\circ$ .

Sablik [19] has advanced a mathematical model and predicted results for maximum flux density  $B_{max}$  and remanence as a function of stress for five different angular orientations between the magnetic field and stress axis. The trend of maximum flux density  $B_{max}$  predicted by Sablik was similar to the trend of  $B_Z$  in this paper. Under tension, for magnetic field applied at angles of  $0^\circ$ ,  $22.5^\circ$ ,  $45^\circ$ , and  $67.5^\circ$  to the stress axis, the  $B_Z$  magnetic signals increase with increasing stress, but the amplitude and monotonicity at these angles are inconsistent with results predicted by the model. For the magnetic field applied at  $90^\circ$  to the stress axis, the  $B_Z$  magnetic signals decrease with increasing stress.

### 3. Conclusions

Based on the experimental results, we can draw the following conclusions:

- (1) The  $B_Z$  distribution of the unloaded specimens is different when the DC magnetic field is applied both parallel and perpendicular to stress, which is caused by the shape anisotropy.
- (2) The amplitude of  $B_Z$  increases with an increase in stress from 0 MPa to 120 MPa when stress is parallel to the DC magnetic field. On the contrary, the amplitude of  $B_Z$  decreases with an increase in stress from 0 MPa to 120 MPa when stress is perpendicular to the DC magnetic field. This phenomenon can be explained by the fact that stress promotes the distribution of magnetic domains in the stress direction.
- (3) Stress parallel to the magnetic field has relatively little effect on the magnetic signals of  $B_Z$ , but stress perpendicular to the magnetic field reduces the magnetic signals of  $B_Z$  considerably.
- (4) There was no shift in the direction of  $B_Z$  variations when the specimens were magnetized parallel to the direction of stress ( $0^\circ$  and  $180^\circ$ ), whereas the direction of  $B_Z$  variations shifted a slight angle relative to the DC magnetic field when the specimens were magnetized perpendicular to the direction of stress ( $90^\circ$  and  $270^\circ$ ).

Further research will be focused on two aspects: (1) the influences of fixed stress and changing magnetic field on magnetic properties of ferromagnetic materials at different angles between the magnetic field and stress axis, such as  $0^\circ$ ,  $22.5^\circ$ ,  $45^\circ$ ,  $67.5^\circ$ , and  $90^\circ$  and (2) the influences of stable magnetic field and varying stress on magnetic properties of ferromagnetic materials at different angles between the magnetic field and stress axis.

**Author Contributions:** Writing—original draft preparation, B.Y.; writing—review and editing, Y.G., L.L. and Z.L.; data curation, R.W.; project administration, Y.Y.; funding acquisition, Y.G. All authors have read and agreed to the published version of the manuscript.

**Funding:** This research was funded by the Ningxia Second-Class Discipline and Scientific Research Projects (Electronic Science and Technology, Grant No. DKPD2022B03) and the Graduate Innovation Project of North Minzu University (Grant No. YCX22125).

**Data Availability Statement:** Not applicable.

**Conflicts of Interest:** The authors declare no conflict of interest.

## References

1. Bulte, D.P.; Langman, R.A. Origins of the magnetomechanical effect. *J. Magn. Magn. Mater.* **2002**, *251*, 229–243. [[CrossRef](#)]
2. Jiles, D.C. Theory of the magnetomechanical effect. *J. Phys. D Appl. Phys.* **1995**, *28*, 1537–1546. [[CrossRef](#)]
3. Jiles, D.C.; Atherton, D.L. Theory of ferromagnetic hysteresis. *J. Magn. Magn. Mater.* **1986**, *61*, 48–60. [[CrossRef](#)]
4. Sablik, M.J.; Kwun, H.; Burkhardt, G.L.; Jiles, D.C. Model for the effect of tensile and compressive stress on ferromagnetic hysteresis. *J. Appl. Phys.* **1987**, *61*, 3799–3801. [[CrossRef](#)]
5. Jiles, D.C.; Li, L. A new approach to modeling the magnetomechanical effect. *J. Appl. Phys.* **2004**, *95*, 7058–7060. [[CrossRef](#)]
6. Hauser, H.; Jiles, D.C.; Melikhov, Y.; Li, L.; Grössinger, R. An approach to modeling the dependence of magnetization on magnetic field in the high field regime. *J. Magn. Magn. Mater.* **2005**, *300*, 273–283. [[CrossRef](#)]
7. Sablik, M.J.; Augustyniak, B.; Chmielewski, M. Modeling biaxial stress effects on magnetic hysteresis in steel with the field and stress axes noncoaxial. *J. Appl. Phys.* **1999**, *85*, 4391–4393. [[CrossRef](#)]
8. Li, L.; Jiles, D.C. A new model equation for interpreting the magnetomechanical effect using generation of the Rayleigh law. In *AIP Conference Proceeding*; American Institute of Physics: College Park, MD, USA, 2003; Volume 657, pp. 1539–1544.
9. Craik, D.J.; Wood, M.J. Magnetization changes induced by stress in a constant applied field. *J. Phys. D Appl. Phys.* **1970**, *3*, 1009–1016. [[CrossRef](#)]
10. Bao, S.; Lou, H.; Gong, S. Magnetic field variation of a low-carbon steel under tensile stress. *Insight Non-Destr. Test. Cond. Monit.* **2014**, *56*, 252–263. [[CrossRef](#)]
11. Pengju, G.; Xuedong, C.; Weihe, G.; Huayun, C.; Heng, J. Effect of tensile stress on the variation of magnetic field of low-alloy steel. *J. Magn. Magn. Mater.* **2011**, *323*, 2474–2477. [[CrossRef](#)]
12. Lihong, D.; Binshi, X.; Shiyun, D.; Qunzhi, C.; Dan, W. Variation of stress-induced magnetic signals during tensile testing of ferromagnetic steels. *NDT&E Int.* **2008**, *41*, 184–189.
13. En, Y.; Xing, C. Magnetic field aberration induced by cycle stress. *J. Magn. Magn. Mater.* **2007**, *312*, 72–77. [[CrossRef](#)]
14. Yang, B.; Li, H.; Zhang, A. Influences of non-coaxial magnetic field on magneto-mechanical effect of ferromagnetic steel. *Int. J. Appl. Electromagn. Mech.* **2019**, *59*, 247–254. [[CrossRef](#)]
15. Bao, S.; Hu, S.N.; Lin, L.; Gu, Y.B.; Fu, M.L. Experiment on the relationship between the magnetic field variation and tensile stress considering the loading history in U75V rail steel. *Insight Non-Destr. Test. Cond. Monit.* **2015**, *57*, 683–688. [[CrossRef](#)]
16. Buschow, K.H.J.; Boer, F.R. *Physics of Magnetism and Magnetic Materials*, 2nd ed.; World Publishing Corporation: Beijing, China, 2013; p. 79.
17. Aharoni, A. Demagnetizing factors for rectangular ferromagnetic prisms. *J. Appl. Phys.* **1998**, *83*, 3432–3434. [[CrossRef](#)]
18. Yamasaki, T.; Yamamoto, S.; Hirao, M. Effect of applied stresses on magnetostriction of low carbon steel. *NDT&E Int.* **1996**, *29*, 263–268.
19. Sablik, M.J.; Rubin, S.W.; Riley, L.A.; Jiles, D.C.; Kaminski, D.A.; Biner, S.B. A model for hysteresis magnetic properties under the application of noncoaxial stress and field. *J. Appl. Phys.* **1993**, *74*, 480–488. [[CrossRef](#)]